NeuroImage: Clinical 46 (2025) 103788

Contents lists available at ScienceDirect

NeuroImage: Clinical

journal homepage: www.elsevier.com/locate/ynicl

Striato-cortical connectivity patterns predict clinical profiles in Huntington's disease

Audrey E. De Paepe [a,b], Vasiliki Bikou [a], Eylül Turan [c], Alexis Pérez-Bellido [b,d,e], Clara Garcia-Gorro [a,b], Nadia Rodriguez-Dechicha [f], Irene Vaquer [f], Matilde Calopa [g], Ruth de Diego-Balaguer [a,b,e,h], Estela Camara [a,*]

[a] Cognition and Brain Plasticity Unit [Bellvitge Biomedical Research Institute – IDIBELL], 08097 L'Hospitalet de Llobregat, Barcelona, Spain
[b] Department of Cognition, Development and Education Psychology, Universitat de Barcelona, Barcelona, Spain
[c] Faculty of Psychology and Educational Sciences, Parenting and Special Education, KU Leuven, Belgium
[d] Department of Cognition, Development and Education Psychology. University Autonoma of Barcelona, Spain
[e] Institute of Neurosciences, Universitat de Barcelona, Barcelona, Spain
[f] Hospital de Día Neurological Diseases Hestia Duran i Reynals, Hospital Duran i Reynals, Hospitalet de Llobregat (Barcelona), Spain
[g] Movement Disorders Unit, Neurology Service, Hospital Universitari de Bellvitge, Barcelona, Spain
[h] ICREA (Catalan Institution for Research and Advanced Studies), Barcelona, Spain

ARTICLE INFO

Keywords:
Huntington's disease
Individual differences
Clinical profiles
rs-fMRI
Principal component analysis

ABSTRACT

Background: Huntington's disease is an inherited neurodegenerative disorder affecting striato-cortical circuits, with significant heterogeneity in the severity and progression of symptoms and neurodegenerative patterns.
Objectives: To identify how distinct functional striato-cortical connectivity signatures may predict clinical profiles in Huntington's disease.
Methods: Thirty-eight Huntington's disease gene expansion carriers underwent cross-sectional motor, cognitive, and behavioral assessments and multimodal MRI. Principal component analysis was employed to characterize Huntington's disease clinical profiles. Next, seed-based whole-brain functional connectivity maps were derived for three basal ganglia seeds (caudate nucleus, putamen, nucleus accumbens) to delineate cortico-striatal connections. Multiple linear regressions assessed relationships between resulting clinical profiles and seed-based resting-state functional connectivity maps. Finally, basal ganglia gray matter volumes were examined in relation to clinical profiles and connectivity.
Results: Principal component analysis identified two main clinical profiles in Huntington's disease: motor-cognitive and behavioral. Multiple linear regression models revealed distinct functional neural signatures associated with each profile. Motor-cognitive symptoms related with a divergent connectivity pattern, specifically decreased connectivity between the caudate and putamen with executive and premotor areas, in contrast to increased connectivity between the ventral nucleus accumbens and executive network regions. Meanwhile, the behavioral profile was linked to decreased connectivity in limbic networks. Basal ganglia atrophy was associated with increased nucleus accumbens-cortical connectivity as well as motor-cognitive symptom severity.
Conclusions: Distinct Huntington's disease clinical profiles can be characterized by predominantly motor-cognitive or behavioral disturbances, each related with unique functional and structural brain signatures. This substantiates that striato-cortical circuits exhibit functional interaction and potential reorganization.

1. Introduction

Huntington's disease (HD) is an inherited, progressive neurodegenerative disease caused by a cytosine-adenine-guanine (CAG) trinucleotide repeat expansion in the *HTT* gene (MacDonald et al., 1993). Despite its monogenic etiology, HD demonstrates significant

Abbreviations: CAG, cytosine-adenine-guanine; HD, Huntington's disease; PCA, principal component analysis; UHDRS, Unified Huntington's Disease Rating Scale.

* Corresponding author at: Cognition and Brain Plasticity Unit, IDIBELL (Institut d'Investigació Biomèdica de Bellvitge), Feixa Larga S/N, 08907 L'Hospitalet de Llobregat, Barcelona, Spain.
E-mail address: ecamara@idibell.cat (E. Camara).

https://doi.org/10.1016/j.nicl.2025.103788
Received 8 January 2025; Received in revised form 28 March 2025; Accepted 15 April 2025
Available online 16 April 2025

heterogeneity in the age of onset and clinical presentation of motor, cognitive, and psychiatric symptoms. This produces diverse disease trajectories among affected individuals, even between monozygotic twins (Georgiou et al., 1999). For example, certain patients exhibit motor symptoms at disease onset, but with minimal mood changes (Kim et al., 2015). Others may present with psychiatric and/or cognitive alterations in the absence of motor symptoms, with involuntary movements emerging later (Considine et al., 2023; Vinther-Jensen et al., 2014). Still others may experience motor, mood, and cognitive symptoms simultaneously, further underscoring the heterogeneous nature of HD (Waldvogel et al., 2012). This variability suggests distinct clinical profiles in HD. However, the relationships between symptom domains remain poorly understood, as does the extent to which specific symptoms are associated within certain profiles or how these associations evolve with brain structure and function.

Neurodegeneration in HD initially affects striato-cortical circuits (Tabrizi et al., 2013; Aylward et al., 2011; Domínguez Duque et al., 2013; Zeun et al., 2019; Zhang et al., 2018; Aylward et al., 2004; Georgiou-Karistianis et al., 2013; Douaud et al., 2009) beginning in the premanifest phase (McColgan et al., 2015; Niccolini and Politis, 2014). This degeneration likewise exhibits individual differences in regional and temporal changes, potentially explaining the observed clinical variability. For example, brain atrophy and cellular loss in the cerebral cortex is regionally heterogeneous (Waldvogel et al., 2014; Vonsattel et al., 1985), and distinct patterns of cortical thinning were associated with differing motor-manifest phenotypes (i.e., bradykinesia/rigidity/dystonia- vs. chorea-predominant), while striatal volumes remained similar (Rosas et al., 2008). At a cellular level, impairments within neuronal populations have been linked with unique clinical profiles in HD, such as specific patterns of neuronal loss associated with motor, mood, and mixed (motor and mood) profiles (Mehrabi et al., 2016; Nana et al., 2014; Thu et al., 2010; Tippett et al., 2007). Meanwhile, Garcia-Gorro et al. (2019) employed a multivariate multimodal structural neuroimaging approach and identified unique neurobiological signatures associated with two different symptom profiles (Garcia-Gorro et al., 2019). Cognitive and motor symptoms were linked to reductions in gray matter volume, cortical thickness, and white matter integrity within cognitive and motor territories; conversely, depressive symptoms were characterized by reduced cortical thickness in limbic and paralimbic regions. However, these studies have focused on linking neural patterns to isolated symptoms rather than considering the complete clinical profile of HD. This narrow focus limits understanding of how different networks and symptom domains interact and overlap.

More generally, modulations of functional and microstructural connectivity have been related with symptom variability in both premanifest and manifest HD across motor, cognitive, and psychiatric domains (De Paepe et al., 2019; Garcia-Gorro et al., 2018; Garcia-Gorro et al., 2019; Harrington et al., 2016; Müller et al., 2016; Odish et al., 2015; Poudel et al., 2014; Quarantelli et al., 2013; Werner et al., 2014; Wolf et al., 2014; Novak et al., 2015). Interestingly, HD exhibits divergent spatiotemporal connectivity patterns, with increased resting-state connectivity observed in the sensory-motor network and decreased connectivity in the executive network (Gregory and Scahill, 2018; Pini et al., 2020). Of note, an increase in functional connectivity, particularly when coupled with preserved motor or cognitive performance despite brain atrophy, is proposed as evidence of compensatory mechanisms or potential brain reorganization in HD (Gregory et al., 2017; Gregory et al., 2018; Klöppel et al., 2015; Soloveva et al., 2018; Soloveva et al., 2020; Pini et al., 2020).

Given the early and striking striatal degeneration in HD coupled with disruptions in structural and functional connectivity, one source of symptom variability may lie in the differential neurodegeneration of distinct striato-cortical circuits. The striato-cortical circuits are comprised of sensory-motor (putamen to motor, premotor, and sensorimotor areas), associative (caudate to dorsolateral and ventrolateral prefrontal cortices), and limbic networks (ventral striatum/nucleus accumbens to orbitofrontal, ventromedial prefrontal, and anterior cingulate cortices) (Haber, 2016). While each of these circuits has distinct functions (e.g., associative with executive functioning and limbic with reward and emotional processing), inter-network interactions regulate motor, cognitive, and limbic functions, extending to resting-state networks (Choi et al., 2012). Diffusion-weighted magnetic resonance imaging studies in humans have confirmed the existence of partially overlapping projections within these striato-cortical loops (Draganski et al., 2008), exemplifying the crucial role that the striatum plays as a hub for motor, cognitive, and behavioral integration (Averbeck et al., 2014). Studying functional alterations both within and between networks is critical to better predict clinical deficits or preserved performance, rather than focusing solely on connectivity imbalances within a single network (Zhang and Pini, 2024).

As such, the present study aimed to examine the dimensionality of clinical profiles in HD and explore the underlying neural patterns. This was carried out by investigating resting-state functional striato-cortical interactions across motor, cognitive, and limbic circuits, which may underlie individual differences in symptom domains.

First, principal component analysis of motor, cognitive, and behavioral clinical variables was employed to characterize symptomatic profiles in HD. Second, multiple linear regressions with seed-based resting-state functional MRI connectivity metrics were performed to predict the severity of the resulting clinical profiles. Seeds of interest comprised the caudate nucleus, putamen, and nucleus accumbens. We hypothesized that striato-cortical brain network connectivity alterations (e.g., heightened or reduced brain activation) may explain symptom variability. Lastly, structural brain atrophy analysis further explored the nature of connectivity patterns and clinical symptoms.

2. Methods

2.1. Participants

Thirty-eight HD gene-expansion carriers (20 manifest, 18 premanifest) participated in the current cross-sectional study (Age: 44.40 $\pm$ 11.38 years; Education: 12.16 $\pm$ 3.18 years; Sex: 25 female, 13 male). HD gene-expansion carriers possessed $\geq$ 39 CAG repeats. Although manifest HD is clinically diagnosed based on motor onset, cognitive, psychiatric, and functional disturbances can present before motor symptoms (Martinez-Horta et al., 2016; Thompson et al., 2012). As such, while not all participants demonstrated motor symptoms, each was a confirmed CAG gene-expansion carrier (43.97 $\pm$ 3.03 CAG repeats). In this way, we studied the disease as a continuum, consistent with previous literature (Aracil-Bolaños et al., 2022).

No participants reported history of a traumatic brain injury or neurological disorder other than HD. The study was approved by the ethics committee of the Bellvitge Institute for Biomedical Research (IDIBELL) and Bellvitge Hospital in accordance with the Helsinki Declaration of 1975. All participants signed written informed consent.

2.2. Clinical evaluation

Three clinical domains (i.e. motor, cognitive, and behavioral) were evaluated (Table 1). Specifically, motor symptoms comprised subdomains of the Unified Huntington's Disease Rating Scale (UHDRS) (Huntington Study Group, 1996). The cognitive domain included measures of cognitive flexibility (Trail Making Test B-A (Tombaugh, 2004), the Boston Naming Test (Kaplan et al., 1983), and cognitive domains of the UHDRS, namely measures of phonemic verbal fluency (F-A-S test) and processing speed and sustained attention (Symbol Digit Modalities Test, word-reading and color-naming components of the Stroop Test). Lastly, behavioral disturbances included the short-Problem Behavioral Assessment (McNally et al., 2015) domains (depressed mood, suicidal ideation, anxiety, apathy, perseveration, obsessive–compulsive behaviors, delusions, hallucinations) and the Sensitivity to Punishment and

Table 1
Clinical and neuroimaging characteristics of Huntington's disease gene-expansion carriers.

	Mean ± Standard deviation	Minimum	Maximum
Motor			
Oculomotor	2.82 ± 3.7	0	11
Dystonia	0.50 ± 0.9	0	3
Chorea	2.74 ± 3.5	0	13
Parkinsonism	2.71 ± 2.9	0	9
Residual motor	1.61 ± 2.0	0	7
Nine-Hole Peg Test	24.89 ± 6.0	15.50	39.75
Cognitive			
Verbal fluency (F-A-S Test)	32.68 ± 13.9	14	69
Symbol Digit Modality Test	37.70 ± 14.8	12	65
Stroop word	77.60 ± 24.2	31	143
Stroop color	57.54 ± 18.6	6	98
TMT B-A	109.09 ± 86.6	10	356
Boston Naming Test	52.47 ± 3.8	41	59
Behavioral			
Depressed mood	1.62 ± 2.8	0	12
Suicidal ideation	0.46 ± 1.4	0	6
Anxiety	1.30 ± 1.9	0	6
Apathy	3.73 ± 4.6	0	16
Perseveration	2.68 ± 3.8	0	16
Obsession-compulsion	0.87 ± 2.3	0	12
Delusions	0.62 ± 2.7	0	16
Hallucinations	0.16 ± 0.7	0	4
Sensitivity to Punishment	10.60 ± 6.3	0	23
Sensitivity to Reward	6.62 ± 3.8	0	15
Gray matter volume*			
Caudate nucleus	$1.64 \times 10^{-3} \pm 4.26 \times 10^{-4}$	8.56×10^{-4}	2.5×10^{-3}
Putamen	$2.12 \times 10^{-3} \pm 5.50 \times 10^{-4}$	1.28×10^{-3}	3.41×10^{-3}
Nucleus accumbens	$1.94 \times 10^{-4} \pm 4.84 \times 10^{-5}$	9.20×10^{-5}	3.08×10^{-4}

*Averaged MRI volume across right and left hemispheres for each participant, normalized for Total Intracranial Volume.
TMT = Trail Making Test B-A.

Sensitivity to Reward Questionnaire (Torrubia et al., 2001).

2.3. MRI data acquisition and processing

MRI data were acquired through a 3 T whole-body MRI scanner (Siemens Magnetom Trio; Hospital Clinic, Barcelona), equipped with a 32-channel phased array head coil. Structural images were assessed using conventional high-resolution 3D T1-weighted images, using a three-dimensional Magnetization Prepared Rapid Gradient Echo (MP-RAGE) sequence (TR = 1970 ms; TE = 2.34 ms; TI = 1050 ms; flip angle = 9°; 1 mm isotropic voxels; 208 sagittal slices; matrix = 208 × 256 × 256; FOV = 256 with no gap between slices). Next, resting-state fMRI images were acquired with a gradient echo-planar imaging sequence (150 volumes; 30 axial slices; 3 mm in-plane resolution; 4 mm thickness; no gap; TR = 2000 ms; TE = 29 ms; flip angle = 80°; FOV = 256 mm).

Please see Supplementary Material for structural MRI preprocessing methods.

With regards to resting-state fMRI, preprocessing and first-level analysis of fMRI data were conducted with the CONN-fMRI Functional Connectivity toolbox v1.2 (www.nitrc.org/projects/conn, RRID: SCR_009550) using standard pipeline protocols. Slice-timing correction was applied, followed by realignment of functional images to the first volume using rigid body spatial transformations to correct for motion artifacts. Next, structural images were co-registered with functional images. Images were spatially normalized to MNI space and resliced to a 2-mm isotropic resolution and then smoothed using an isotropic Gaussian kernel (FWHM = 8 mm). To minimize potential confounding effects, we used ART-based scrubbing to detect and exclude motion related outlier volumes. Additionally, during denoising, we regressed out twelve motion-related covariates (six motion parameters and six temporal derivatives), along with white matter and cerebrospinal fluid physiological noise sources (Behzadi et al., 2007). Lastly, images were band-pass filtered (0.01 Hz ~ Inf) to attenuate low frequency drift and high-frequency noise artifacts. The average translation was 0.05 mm (SD = 0.03 mm) and the average rotation was 0.0008° (SD = 0.0005°).

2.4. Statistical analysis

2.4.1. Clinical data dimensionality

Statistical analysis was carried out in R v. 4.3.3 (R Foundation for Statistical Computing, Vienna, Austria). Clinical data were 90 % winsorized to reduce the effect of outliers and then standardized to *Z*-scores. Missing values for behavioral variables were replaced by their mean. Specific cognitive measures were reverse scored (i.e., multiplied by −1) so that a more positive score indicated more severe symptoms for all domains. To identify different clinical profiles, we conducted principal component analysis (PCA) (no rotation) on the clinical data of HD patients, with twenty-two variables for inclusion. The data satisfied conventional requirements for factor analysis with the Kaiser-Meyer-Olkin measure of sampling adequacy and Bartlett's test of sphericity.

Main components were extracted based on eigenvalues > 1 and percent variance explained > 10 %. These components explained the majority of variance (i.e., $\geq$50 % cumulative variance). Extraction communality values illustrate the estimated variance of each item accounted for by the extracted factors. Individual patient's loading scores on each extracted factor were then used as clinical profile variables in the multiple linear regression neuroimaging analysis.

2.4.2. Seed-based resting-state fMRI connectivity and relationship with clinical profiles

First, we computed the mean time series for each basal ganglia seed. Seeds for functional connectivity analysis were bilaterally defined in the caudate nucleus, putamen, and nucleus accumbens using the Automated Anatomical Labeling (AAL) (https://www.gin.cnrs.fr/en/tools/aal/). Then, for each seed region, voxel-based Pearson correlation coefficients were calculated between the mean time series of the seed and the time series of all other voxels in the brain. These correlation coefficients were transformed into normally distributed Z-scores using Fisher's transformation and were bilaterally averaged. Subsequently, the seed-based connectivity maps of individual patients were entered into a one-sample *t*-test to identify main connectivity effects for each seed.

Significant results for each seed-based striato-cortical connectivity analysis were reported using a threshold of $P \leq 0.05$ with family-wise error correction for multiple comparisons at the whole-brain level.

Next, separate multiple linear regression models were created, corresponding to each of the main components of the PCA analysis. These models employed the loading scores of the extracted factors of the PCA as the dependent variable and the seed-based connectivity maps (caudate, putamen, nucleus accumbens) as independent variables.

Statistical significance was identified at $P < 0.001$ and corrected for multiple comparisons at cluster level ($P \leq 0.05$), with a minimum cluster size of $k = 10$ contiguous voxels. The maxima of suprathreshold regions were rendered onto a T1 structural template-image on the MNI reference brain for localization. Anatomic areas were identified using the Automated Anatomical Labeling Atlas included in the xjView toolbox (https://www.alivelearn.net/xjview).

2.5. Data availability statement

The raw data supporting the findings of this study cannot be shared publicly as they contain clinical and genetic information sensitive to the Institution. In the interest of minimizing the risk of participant identification, we will make the data available upon reasonable request to the corresponding author (ecamara@idibell.cat), with approval by the local institutional review board.

3. Results

3.1. Dimensionality of clinical profiles in HD

The data met the basic requirements for factor analysis per the Kaiser-Meyer-Olkin measure of sampling adequacy (KMO = 0.682) and Bartlett's test of sphericity ($P < 0.001$). PCA resulted in six components with eigenvalues > 1 (Table S1). Of these, two main principal components cumulatively explained 50.6 % of variance and were thus the focus of further analyses. The first component (PC1) was robustly associated with motor-cognitive measures and explained 35.0 % of the variance, while the second component (PC2) consisted of behavioral measures, explaining 15.6 % of variance (Table 2; Fig. 1). Higher values reflect more severe dysfunction in that domain.

3.2. Resting-state connectivity maps of basal ganglia seeds

Whole-brain resting-state functional connectivity maps for each basal ganglia seed engaged well-established striato-cortical circuits (Table S2; Fig. S1). The caudate nucleus demonstrated connectivity with regions of executive networks, including the superior and medial frontal gyri, the dorsolateral prefrontal cortex, and the dorsal anterior cingulate; the putamen exhibited connectivity with motor, premotor, and sensorimotor regions, such as the supplementary motor area and precentral gyrus; lastly, the nucleus accumbens was associated with more ventral limbic connections, namely the orbitofrontal cortex, ventral anterior cingulate, and insula.

Table 2
Principal component analysis of clinical assessment items (motor, cognitive, behavioral), component matrix.

Item*	EC	Component loadings	
		PC1: Motor-Cognitive	PC2: Behavioral
Oculomotor	0.746	**0.827**	0.037
Dystonia	0.740	**0.791**	−0.017
Chorea	0.634	**0.721**	−0.110
Parkinsonism	0.802	**0.851**	−0.003
Residual motor	0.751	**0.806**	−0.220
Nine-Hole Peg Test	0.691	**0.786**	0.096
Verbal fluency (F-A-S Test)	0.756	**0.718**	0.159
Symbol Digit Modality Test	0.788	**0.883**	0.031
Stroop word	0.824	**0.810**	0.036
Stroop color	0.670	**0.684**	0.174
TMT	0.683	**0.788**	0.018
Boston Naming Test	0.764	**0.685**	0.075
Depressed mood	0.862	−0.307	**0.796**
Suicidal ideation	0.938	−0.263	**0.675**
Anxiety	0.804	−0.232	0.315
Apathy	0.863	0.195	**0.729**
Perseveration	0.699	0.133	**0.763**
Obsession-compulsion	0.752	−0.004	**0.448**
Delusions	0.805	−0.127	**0.446**
Hallucinations	0.809	−0.071	**0.538**
Sensitivity to Punishment	0.828	0.182	0.324
Sensitivity to Reward	0.787	0.223	**0.449**
% Variance	–	35.0 %	15.6 %

Factor loadings > 0.40 are highlighted in **bold**.
EC = extraction communality values; PC = principal component; TMT = Trail Making Test.

3.3. Relationship between functional connectivity and clinical profiles

Next, we investigated whether the two identified clinical profiles in HD (i.e., extracted principal components) were associated with specific neural functional connectivity signatures. To achieve this, two separate multiple linear regression models were performed, one for each main principal component (dependent variable), with the three basal ganglia seeds (caudate nucleus, putamen, nucleus accumbens) serving as independent variables (see Methods).

Functional connectivity analyses are presented for each seed (Table 3). Greater deficits in the motor-cognitive domain (PC1) were associated with altered connectivity between the three basal ganglia seeds and partially overlapping cortical networks, with dorsal striatal regions showing a decrease in connectivity and the nucleus accumbens exhibiting an increase in connectivity. Specifically, the putamen demonstrated reduced functional connectivity with the premotor network, particularly the supplementary motor area. The caudate nucleus showed reduced connectivity with the executive and premotor networks for PC1, encompassing cortical nodes such as the superior and medial frontal cortices extending to the supplementary motor area, as well as the left middle temporal lobe and parietal regions (Fig. 2). In contrast, the nucleus accumbens exhibited a significant increase in connectivity between similar executive networks, spanning territories such as the dorsolateral prefrontal cortex, medial frontal gyrus, and angular gyrus (Fig. 2). In terms of the behavioral dimension (PC2), decreased connectivity was found between the putamen and limbic networks.

3.4. Gray matter volume analysis

To better understand the divergent connectivity pattern of the main motor-cognitive profile, gray matter volumes of the three basal ganglia seeds (caudate nucleus, putamen, nucleus accumbens) were correlated with the principal component factor loading scores for each participant as well as the connectivity values between the nucleus accumbens and the corresponding cortical regions-of-interest. Due to non-normality (Shapiro-Wilks test), Spearman's rho was used. Correlations were corrected using the false discovery rate, where P-adjusted (P-adj) ≤ 0.05 was considered significant. Both raw P values and P-adj are reported.

Gray matter volumes of the three basal ganglia seeds showed a significant negative relationship with the motor-cognitive profile (PC1) (Fig. S2A). Specifically, more severe scores in the motor-cognitive dimension were associated with decreased gray matter volume in the caudate nucleus ($r = -0.803$, $P < 0.001$, P-adj < 0.001), putamen ($r = -0.780$, $P < 0.001$, P-adj < 0.001), and nucleus accumbens ($r = -0.715$, $P < 0.001$, P-adj < 0.001). Moreover, individuals with lower gray matter volume in the basal ganglia exhibited a greater increase in functional connectivity between the nucleus accumbens and executive network (Fig. S2B). This relationship was significant in the caudate nucleus ($r = -0.359$, $P = 0.027$, P-adj $= 0.041$) and nucleus accumbens ($r = -0.333$, $P = 0.041$, P-adj $= 0.049$).

4. Discussion

This study examined the clinical profiles of individuals with HD and their associations with striato-cortical resting-state functional connectivity patterns. Two distinct profiles were revealed: one characterized by motor and cognitive deficits, and the other by behavioral impairments. Analysis of striato-cortical networks indicated that these clinical profiles corresponded to unique and divergent connectivity patterns. The motor-cognitive profile accounted for the majority of variance and was associated with both decreased connectivity from the dorsal striatum (caudate nucleus and putamen) and increased connectivity from the nucleus accumbens to a broad network encompassing frontal, parietal, and temporal connections. In contrast, the behavioral profile showed a more focused reduction in connectivity, primarily involving limbic brain

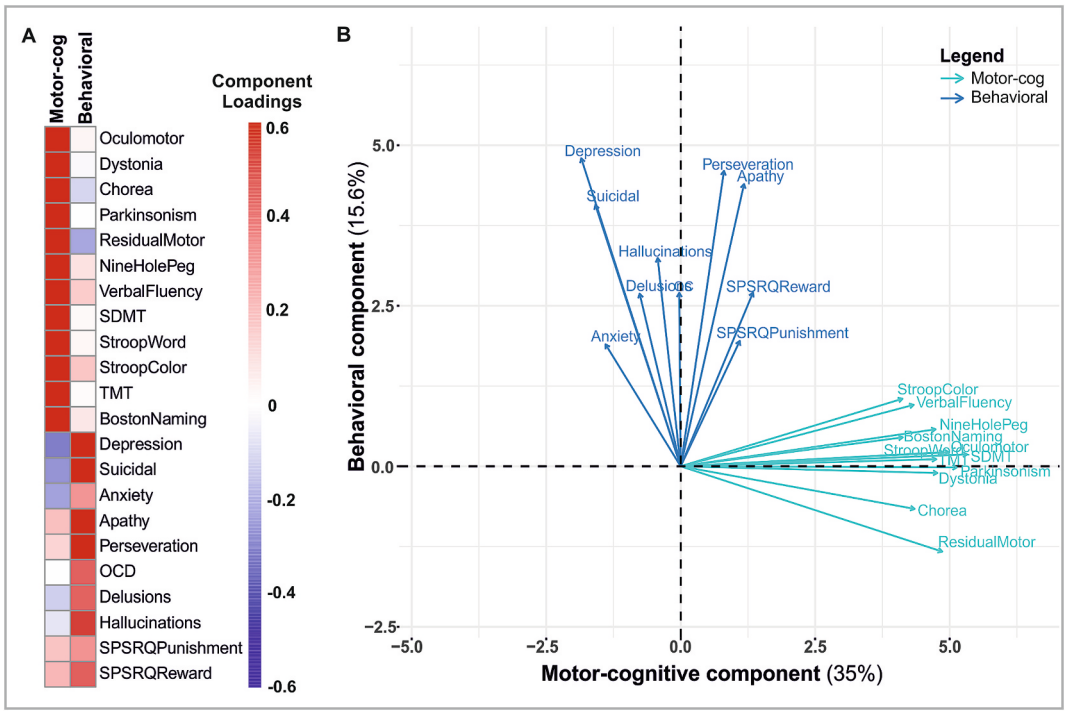

Fig. 1. Principal component analysis of clinical assessment items produced two main clinical profiles: motor-cognitive (PC1) and behavioral (PC2). **(A)** Component loadings of motor, cognitive, and behavioral variables on two main components. **(B)** Principal component analysis of projected weights (lengths) and correlations (directions) for each variable on two main components, with explained variance additionally indicated for each component (%).

regions.

To date, few studies have subdivided patients into distinct profiles based on neuroimaging metrics and phenotypic variability. One multivariate multimodal neuroimaging study in a related cohort examined the neurobiological basis of interindividual differences and demonstrated that cognitive-motor and psychiatric symptom profiles show distinct patterns of brain changes (Garcia-Gorro et al., 2019). Another recent study examining 46 behavioral, cognitive, and motor phenotypic variables identified two principal components in HD: the first comprised cognitive, motor, and functional domains, while the second encompassed behavioral variables (Fitt et al., 2024). These findings underscore a distinction between motor-cognitive and behavioral profiles in HD and align with the present results.

Notably, this study identified divergent patterns of connectivity directionality related to the motor-cognitive phenotype, which originated from the dorsal striatum and nucleus accumbens. This suggests potential reorganization and interaction between topologically segregated networks in HD. Previous research using a mixed premanifest and manifest HD sample reported similar findings, showing reduced connectivity between the premotor cortex and the striatum in relation to increased motor symptoms (Kronenbuerger et al., 2019). Reduced striato-cortical connectivity between the caudate and premotor areas has been previously shown in a sample of premanifest HD individuals, although the relationship with clinical symptoms was not examined (Unschuld et al., 2012). Similarly using a seed-based approach, decreased connectivity within the motor network was associated with poorer motor abilities (Müller et al., 2016). However, the authors didn't specifically assess striato-cortical connections. Also in line with our results, motor symptomatology seems to be related to brain regions outside of the motor network, including the superior and inferior parietal cortices and precuneus (Werner et al., 2014).

In contrast, several studies using whole-brain independent component analysis observed increased connectivity within the motor network in manifest or combined manifest and premanifest HD samples, where higher connectivity correlated with more severe motor impairments (Werner et al., 2014; Wolf et al., 2014). Conversely, in premanifest HD, lower connectivity was associated with worsening motor function (Poudel et al., 2014). Despite methodological differences, these studies collectively suggest that while functional coupling between networks deteriorates as symptoms progress, there may also be increased coactivation within neural networks.

In the frontal and parietal brain regions (i.e., those involved in executive functions), we observed contradictory patterns of striatal connectivity. As motor-cognitive symptom severity increased, we observed a spatial gradient in regions such as the right middle frontal gyrus, right dorsolateral prefrontal cortex, and angular gyrus, where dorsal striatal (i.e., caudate) connections weakened, but ventral striatal (i.e., nucleus accumbens) connections strengthened. Previous studies have reported increased striato-prefrontal connectivity, which was related to greater genetic burden and diminished cognitive performance (Kronenbuerger et al., 2019). In this study, we replicated these findings and further demonstrated that this increase is primarily driven by the nucleus accumbens, rather than the striatum as a whole. This relationship between the motor-cognitive profile and the divergent connectivity pattern may suggest compensatory neural adaptations aimed at mitigating the emerging motor-cognitive impairments, or simply aberrant connectivity that is part of the pathological neurodegenerative process. In this vein, exploratory post-hoc analyses revealed that as the volume of the nucleus accumbens decreased, its cortical connections increased.

Evidence for a possible compensatory functional reorganization can also be understood in light of histopathological evidence of dorsomedial to ventrolateral striatal neurodegeneration (Vonsattel et al., 1985; Paulsen, 2009; Vonsattel et al., 2011). Importantly, in HD, the relative preservation of the ventral striatum and limbic circuitry until later disease stages raises the possibility that these circuits could serve as networks for compensatory strategies, potentially mitigating early deficits in motor and cognitive functions through increasing activation. In this vein, increased activity within more preserved circuits has been linked to maintained performance in motor and cognitive tasks in premanifest and early manifest stages of HD (Gregory et al., 2017; Gregory et al.,

Table 3
Linear regression of basal ganglia resting-state functional connectivity with clinical profiles.

Anatomical region	Hemisphere	Cluster size	T value	*P* value	MNI Coordinates (*x*,*y*,*z*)
Motor-cognitive (PC1)					
Caudate					
SFG/MFG (BA 8)	L	221	−6.02	<0.001	−2 30 56
Premotor cortex (BA 6)	L		−5.66		–22 2 68
SMA (BA 6)	R		−5.06		2 10 64
Premotor cortex (BA 6)	R	36	−5.70	0.001	22 6 64
Middle temporal gyrus(BA 21)	L	29	−5.17	0.002	−66 –42 −4
Middle temporal gyrus(BA 21)	L		−3.69		−62 –30 −8
Superior parietal (BA 7)	R	13	−5.02	0.029	34 –66 56
Cerebellar crus II	R	20	−4.98	0.009	10 –90 −28
Precuneus (BA 7)	R	12	−4.83	0.035	2 –66 48
SFG (BA 8)	R	37	−4.72	0.001	38 22 48
dlPFC (BA 9)	R		−4.36		46 18 44
dlPFC (BA 9)	R		−4.29		42 30 36
Thalamus	L	12	−4.43	0.035	−2 –6 4
Angular gyrus (BA 39)	L	20	−4.41	0.009	−42 –62 40
Inferior parietal (BA 7)	L		−4.25		−38 –62 52
Cerebellum, posterior	R	19	−4.22	0.010	38 –70 −24
Cerebellar crus I	R		−3.85		46 –70 −24
Cerebellum, posterior	R		−3.79		38 –66 −24
Caudate	L	19	+5.53	0.010	−10 14 8
Putamen					
SMA	R	10	−4.44	0.051	6 2 60
Nucleus accumbens					
dlPFC (BA 9)	R	17	+4.70	0.014	46 30 36
Angular gyrus (BA 39)	R	17	+4.13	0.014	54 –70 28
Middle temporal gyrus (BA 39)	R		+4.10		38 –62 28
MFG(BA 8)	R	17	+4.09	0.014	2 34 44
MFG(BA 8)	L		+3.65		−6 30 44
Behavioral (PC2)					
Putamen					
Parahippocampal gyrus	R	13	−4.08	0.029	22 14 –28
Medial OFC (BA 47)	R		−3.49		14 22 –24

BA = Brodmann area; dlPFC = dorsolateral prefrontal cortex; L = left; MFG = medial frontal gyrus; MNI = Montreal Neurological Institute; OFC = orbitofrontal cortex; PC = principal component; R = right; SFG = superior frontal gyrus; SMA = supplementary motor area.

2018; Klöppel et al., 2015; Soloveva et al., 2018; Soloveva et al., 2020). Considering the functional gradient of the prefrontal cortex (Abdallah et al., 2022), putative compensatory mechanisms could still be applied in ventral regions that relate to simpler executive functions, while they are no longer possible for more complex functions relying on dorsal prefrontal cortical areas.

In contrast to the widespread connectivity associated with motor-cognitive deficits, behavioral symptoms were represented by a more limited connectivity network. The increased burden of behavioral issues (i.e., psychiatric disturbances and sensitivity to reward and punishment) was linked to altered connectivity between the putamen and both the parahippocampal gyrus and orbitofrontal cortex. While research on neuropsychiatric disturbances and intrinsic functional connectivity in HD is scarce, these brain regions are implicated in depression and apathy in other neurodegenerative diseases and in the general population (Thobois et al., 2010; Rolls et al., 2020; Benoit et al., 2002). In Parkinson's disease, decreased functional connectivity between the orbitofrontal cortex and parahippocampal gyrus has been associated with neuropsychiatric symptoms (Dan et al., 2017). Similarly, imbalances in orbitofrontal cortex connectivity may contribute to depression, as seen in healthy individuals, where reduced functional connectivity between the medial orbitofrontal cortex and parahippocampal gyrus correlates with depressive symptoms (Rolls et al., 2020). In HD specifically, decreased structural striato-cortical connectivity has been linked to greater depressive symptoms, though this was not consistently observed in functional connectivity analyses, indicating the need for further research to clarify these relationships (McColgan et al., 2017).

These findings have notable implications for the understanding of striato-cortical circuits in HD. Primarily, the two clinical profiles were represented not by isolated disruptions in distinct striato-cortical circuits, but rather by an interplay of divergent connectivity patterns stemming from both dorsal and ventral regions. Overall, the cross-talk between striato-cortical circuits is evidenced by studies showing how specific cortical regions with distinct functions converge within the same striatal structures (Averbeck et al., 2014; Jarbo and Verstynen, 2015). Several additional studies consistently highlight shared neural circuits underlying the connection between cognitive and motor functions (Suzuki et al., 2004; Oliveira et al., 2018; Plummer et al., 2013). Our results further support this cross-talk, demonstrating that striatal circuits don't function in isolation.

Exploring differences in the onset and trajectories over time between the two connectivity patterns is an important avenue for future research. This understanding could yield critical insights into the prognostic implications of each pattern, enabling more accurate predictions of disease progression and facilitating healthcare interventions that aim to sustain functional capacity and delay disturbances across motor-cognitive domains. For example, distinct neural signatures may provide a basis for the selection of patients that may be more likely to benefit from stereotactic intervention, such as the stimulation or potentiation of nodes within disrupted or compensatory networks, providing an alternative clinical approach to forestall disease onset and progression. Additionally, connectivity biomarkers may serve as surrogate outcomes for assessing the effectiveness of clinical interventions in premanifest HD. In summary, these findings further elucidate the identification of specific biomarkers related to clinical profiles in HD, with possible applications in patient selection and treatment assessment in clinical trials.

This study is not without limitations. First, rs-fMRI acquisition parameters were restricted to only 150 volumes and 4 mm slice thickness, with a total scan time of five minutes (TR = 2000 ms and no gap). Second, the lack of control subjects limits our ability to elucidate if the alterations in brain connectivity profiles represent underlying hypo- or hyperconnectivity. For this reason, our study focused on the relationship between divergent connectivity networks and clinical profiles, whereby encompassing both manifest and premanifest patients provides the most comprehensive view of the disease spectrum. Third, while the observed distinction between motor-cognitive and behavioral profiles replicate and extend previous findings in HD (Garcia-Gorro et al., 2019; Fitt et al., 2024), it is possible that other clinical profiles exist. While the motor-cognitive and behavioral components cumulatively explained more than 50 % of the variance, this threshold may have overlooked other clinical patterns. Continued investigation of this research question in larger, multicenter databases, such as Enroll-HD or REGISTRY (Landwehrmeyer et al., 2016; van Duijn et al., 2014), is warranted to potentially delineate additional HD profiles across motor, cognitive, and behavioral domains. Such large datasets could leverage machine learning to identify latent patterns in multimodal data, including PET and electrophysiology data, and future studies can take advantage of

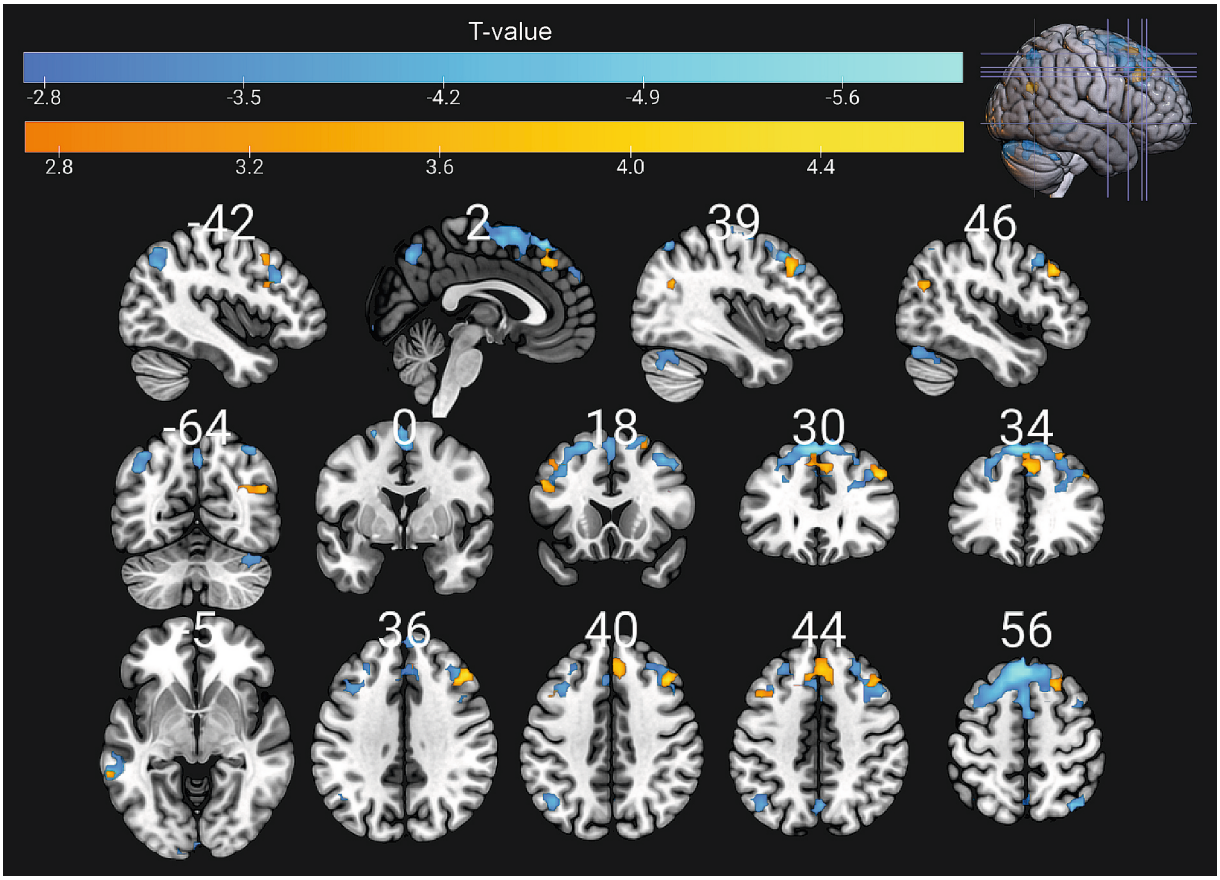

Fig. 2. Functional connectivity regression maps of the motor-cognitive profile, with decreased connectivity for the caudate nucleus (blue) and increased connectivity for the nucleus accumbens (orange). Results illustrated at $P < 0.005$ (uncorrected at voxel-level), $k = 20$. Slice position in MNI coordinates.

active or transfer learning strategies even on smaller datasets to increase speed and accuracy of analysis (Myszczynska et al., 2020; Du et al., 2024).

In summary, clinical heterogeneity in HD may be delineated by distinct clinical profiles of patients characterized by motor-cognitive or behavioral disturbances, each associated with unique patterns of functional and structural brain alterations. In HD, striato-cortical circuits appear to engage in cross-talk and reorganization, potentially serving compensatory mechanisms in response to neurodegeneration. These findings support the recent perspective of functional integration within striato-cortical networks, rather than strict functional segregation. Ultimately, such distinct neural signatures may provide a basis for the identification of connectivity biomarkers to assess the effectiveness of clinical interventions in HD, paving the way for personalized treatment strategies tailored to specific clinical profiles.

CRediT authorship contribution statement

Audrey E. De Paepe: Writing – review & editing, Writing – original draft, Investigation, Formal analysis, Data curation. **Vasiliki Bikou:** Writing – review & editing, Writing – original draft, Data curation. **Eylül Turan:** Writing – review & editing, Writing – original draft, Formal analysis, Data curation. **Alexis Pérez-Bellido:** Writing – review & editing, Methodology. **Clara Garcia-Gorro:** Writing – review & editing, Data curation. **Nadia Rodriguez-Dechicha:** Writing – review & editing, Supervision, Resources, Data curation. **Irene Vaquer:** Writing – review & editing, Data curation. **Matilde Calopa:** Writing – review & editing, Data curation. **Ruth de Diego-Balaguer:** Writing – review & editing, Data curation. **Estela Camara:** Writing – review & editing, Writing – original draft, Supervision, Resources, Funding acquisition, Formal analysis, Data curation, Conceptualization.

Funding

This work was supported by the Instituto de Salud Carlos III, which is an agency of the MINECO, co-funded by FEDER funds/European Regional Development Fund (ERDF) – a way to Build Europe (CP13/00225, PI14/00834, to EC). This study was also funded by AGAUR 2021SGR00352, the Agencia Estatal de Investigación (AEI), an agency of MINECO, and co-funded by FEDER funds/European Regional Development Fund (ERDF) – a Way to Build Europe (number PID2020-114518RB-I00 / DOI: 10.13039/501100011033 to EC, BFU2017-87109-P to RdD). We also thank CERCA Programme/Generalitat de Catalunya for institutional support.

Declaration of competing interest

The authors declare that they have no known competing financial interests or personal relationships that could have appeared to influence the work reported in this paper.

Acknowledgements

We are grateful to the patients and their families for their participation. We would also like to thank Dr. Saül Martinez-Horta, Dra. Andrea Horta-Barba, Dr. Jesús Pérez Pérez, Dr. Jaime Kulisevksy, Pilar Sanchez, Dr. Esteban Muñoz, Celia Mareca, Dr. Ruiz-Idiago for help with clinical evaluation and data collection.

Authors' roles

Audrey E De Paepe: execution, analysis, writing, editing of final version of manuscript.

Vasiliki Bikou: writing, editing of final version of manuscript.

Eylül Turan: writing.

Alexis Pérez-Bellido: analysis.

Clara Garcia-Gorro: execution, editing of final version of the manuscript.

Nadia Rodriguez-Dechicha: execution, editing of final version of the manuscript.

Irene Vaquer: execution, editing of final version of the manuscript.

Matilde Calopa: execution, editing of final version of the manuscript.

Ruth de Diego-Balaguer: design, editing of final version of the manuscript.

Estela Camara: design, execution, analysis, writing, editing of final version of the manuscript.

Financial disclosures

None.

Appendix A. Supplementary data

Supplementary data to this article can be found online at https://doi.org/10.1016/j.nicl.2025.103788.

Data availability

The raw data that support the findings of this study are available from the corresponding author upon reasonable request after approval of local institutional review board.

References

Abdallah, M., Zanitti, G.E., Iovene, V., Wassermann, D., 2022. Functional gradients in the human lateral prefrontal cortex revealed by a comprehensive coordinate-based meta-analysis. Elife 11, e76926. Badre D, Frank MJ, editors.

Aracil-Bolaños, I., Martínez-Horta, S., González-de-Echávarri, J.M., Sampedro, F., Pérez-Pérez, J., Horta-Barba, A., et al., 2022. Structure and dynamics of large-scale cognitive networks in Huntington's disease. Mov. Disord. 37 (2), 343–353.

Averbeck, B.B., Lehman, J., Jacobson, M., Haber, S.N., 2014. Estimates of projection overlap and zones of convergence within frontal-striatal circuits. J. Neurosci. 34 (29), 9497–9505.

Aylward, E.H., Sparks, B.F., Field, K.M., Yallapragada, V., Shpritz, B.D., Rosenblatt, A., et al., 2004. Onset and rate of striatal atrophy in preclinical Huntington disease. Neurology 63 (1), 66–72.

Aylward, E.H., Nopoulos, P.C., Ross, C.A., Langbehn, D.R., Pierson, R.K., Mills, J.A., et al., 2011. Longitudinal change in regional brain volumes in prodromal Huntington disease. J. Neurol. Neurosurg. Psychiatry 82 (4), 405–410.

Behzadi, Y., Restom, K., Liau, J., Liu, T.T., 2007. A component based noise correction method (CompCor) for BOLD and perfusion based fMRI. Neuroimage 37 (1), 90–101.

Benoit, M., Koulibaly, P.M., Migneco, O., Darcourt, J., Pringuey, D.J., Robert, P.H., 2002. Brain perfusion in Alzheimer's disease with and without apathy: a SPECT study with statistical parametric mapping analysis. Psychiatry Res. Neuroimaging 114 (2), 103–111.

Choi, E.Y., Yeo, B.T.T., Buckner, R.L., 2012. The organization of the human striatum estimated by intrinsic functional connectivity. J. Neurophysiol. 108 (8), 2242–2263.

Considine, C.M., Rossetti, M.A., Del Bene, V.A., Anderson, K., Anderson, S.A., Celka, A.S., et al., 2023. Huntington Study Group's Neuropsychology Working Group: Implementing non-motor diagnostic criteria. Mov. Disord. Clin. Pract. 10 (12), 1714–1724.

Dan, R., Růžička, F., Bezdicek, O., Růžička, E., Roth, J., Vymazal, J., et al., 2017. Separate neural representations of depression, anxiety and apathy in Parkinson's disease. Sci. Rep. 7 (1), 12164.

De Paepe, A.E., Sierpowska, J., Garcia-Gorro, C., Martinez-Horta, S., Perez-Perez, J., Kulisevsky, J., et al., 2019. White matter cortico-striatal tracts predict apathy subtypes in Huntington's disease. NeuroImage Clin. 24, 101965.

Domínguez Duque, J.F., Egan, G.F., Gray, M.A., Poudel, G.R., Churchyard, A., Chua, P., et al., 2013. Multi-modal neuroimaging in premanifest and early Huntington's disease: 18 month longitudinal data from the IMAGE-HD study. PLoS One 8 (9), e74131.

Douaud, G., Behrens, T.E., Poupon, C., Cointepas, Y., Jbabdi, S., Gaura, V., et al., 2009. In vivo evidence for the selective subcortical degeneration in Huntington's disease. Neuroimage 46 (4), 958–966.

Draganski, B., Kherif, F., Klöppel, S., Cook, P.A., Alexander, D.C., Parker, G.J.M., et al., 2008. Evidence for Segregated and Integrative Connectivity Patterns in the Human Basal Ganglia. J. Neurosci. 28 (28), 7143–7152.

Du, L., Roy, S., Wang, P., Li, Z., Qiu, X., Zhang, Y., et al., 2024. Unveiling the future: Advancements in MRI imaging for neurodegenerative disorders. Ageing Res. Rev. 95, 102230.

Fitt, D., Wills, C., Massey, T., McLauchlan, D., Holmans, P., 2024. F061 Risk factors associated with cognitive/psychiatric/behavioural phenotypes in Huntington's disease. J. Neurol. Neurosurg. Psychiatry 95 (Suppl 1), A92–A93.

Garcia-Gorro, C., de Diego-Balaguer, R., Martínez-Horta, S., Pérez-Pérez, J., Kulisevsky, J., Rodríguez-Dechicha, N., et al., 2018. Reduced striato-cortical and inhibitory transcallosal connectivity in the motor circuit of Huntington's disease patients: Connectivity of the Motor Circuit in Huntington's Disease. Hum. Brain Mapp. 39 (1), 54–71.

Garcia-Gorro, C., Garau-Rolandi, M., Escrichs, A., Rodriguez-Dechicha, N., Vaquer, I., Subira, S., et al., 2019. An active cognitive lifestyle as a potential neuroprotective factor in Huntington's disease. Neuropsychologia 122, 116–124.

Garcia-Gorro, C., Llera, A., Martinez-Horta, S., Perez-Perez, J., Kulisevsky, J., Rodriguez-Dechicha, N., et al., 2019. Specific patterns of brain alterations underlie distinct clinical profiles in Huntington's disease. NeuroImage Clin. 23, 101900.

Georgiou, N., Bradshaw, J.L., Chiu, E., Tudor, A., O'Gorman, L., Phillips, J.G., 1999. Differential clinical and motor control function in a pair of monozygotic twins with Huntington's disease. Mov. Disord. Off. J. Mov. Disord .Soc. 14 (2), 320–325.

Georgiou-Karistianis, N., Scahill, R., Tabrizi, S.J., Squitieri, F., Aylward, E., 2013. Structural MRI in Huntington's disease and recommendations for its potential use in clinical trials. Neurosci. Biobehav. Rev. 37 (3), 480–490.

Gregory, S., Long, J.D., Klöppel, S., Razi, A., Scheller, E., Minkova, L., et al., 2017. Operationalizing compensation over time in neurodegenerative disease. Brain 140 (4), 1158–1165.

Gregory, S., Scahill, R.I., 2018. Chapter 10. Functional magnetic resonance imaging in Huntington's disease. In: International Review of Neurobiology, pp. 381–408.

Gregory, S., Long, J.D., Klöppel, S., Razi, A., Scheller, E., Minkova, L., et al., 2018. Testing a longitudinal compensation model in premanifest Huntington's disease. Brain 141 (7), 2156–2166.

Haber, S.N., 2016. Corticostriatal circuitry. Dialogues Clin. Neurosci. 18 (1), 15.

Harrington, D.L., Long, J.D., Durgerian, S., Mourany, L., Koenig, K., Bonner-Jackson, A., et al., 2016. Cross-sectional and longitudinal multimodal structural imaging in prodromal Huntington's disease. Mov. Disord. 31 (11), 1664–1675.

Huntington Study Group, 1996. Unified Huntington's disease rating scale: reliability and consistency. Mov. Disord. 11 (2), 136–142.

Jarbo, K., Verstynen, T.D., 2015. Converging structural and functional connectivity of orbitofrontal, dorsolateral prefrontal, and posterior parietal cortex in the human striatum. J. Neurosci. 35 (9), 3865–3878.

Kaplan, E., Goodglass, H., Weintraub, S., 1983. Boston naming test [Internet] [cited 2024 Dec 4]. Available from: Philadelphia: Lee & Febiger https://doi.apa.org/doi/10.1037/t27208-000.

Kim, J., Long, J.D., Mills, J.A., McCusker, E., Paulsen, J.S., 2015. Multivariate clustering of progression profiles reveals different depression patterns in prodromal Huntington disease. Neuropsychology 29 (6), 949–960.

Klöppel, S., Gregory, S., Scheller, E., Minkova, L., Razi, A., Durr, A., et al., 2015. Compensation in preclinical Huntington's disease: Evidence from the Track-On HD study. EBioMedicine 2 (10), 1420–1429.

Kronenbuerger, M., Hua, J., Bang, J.Y.A., Ultz, K.E., Miao, X., Zhang, X., et al., 2019. Differential changes in functional connectivity of striatum-prefrontal and striatum-motor circuits in premanifest Huntington's disease. Neurodegener Dis 19 (2), 78–87.

Landwehrmeyer, G.B., Fitzer-Attas, C.J., Giuliano, J.D., Gonçalves, N., Anderson, K.E., Cardoso, F., et al., 2016. Data analytics from Enroll-HD, a global clinical research platform for Huntington's disease. Mov Disord Clin Pract. 4 (2), 212–224.

MacDonald, M.E., Ambrose, C.M., Duyao, M.P., Myers, R.H., Lin, C., Srinidhi, L., et al., 1993. A novel gene containing a trinucleotide repeat that is expanded and unstable on Huntington's disease chromosomes. Cell 72 (6), 971–983.

Martinez-Horta, S., Perez-Perez, J., van Duijn, E., Fernandez-Bobadilla, R., Carceller, M., Pagonabarraga, J., et al., 2016. Neuropsychiatric symptoms are very common in premanifest and early stage Huntington's Disease. Parkinsonism Relat. Disord. 25, 58–64.

McColgan, P., Seunarine, K.K., Razi, A., Cole, J.H., Gregory, S., Durr, A., et al., 2015. Selective vulnerability of Rich Club brain regions is an organizational principle of structural connectivity loss in Huntington's disease. Brain J. Neurol. 138 (Pt 11), 3327–3344.

McColgan, P., Razi, A., Gregory, S., Seunarine, K.K., Durr, A., Roos, A.C.R., et al., 2017. Structural and functional brain network correlates of depressive symptoms in premanifest Huntington's disease. Hum. Brain Mapp. 38 (6), 2819–2829.

McNally, G., Rickards, H., Horton, M., Craufurd, D., 2015. Exploring the validity of the short version of the Problem Behaviours Assessment (PBA-s) for Huntington's disease: A Rasch analysis. J Huntingt Dis. 4 (4), 347–369.

Mehrabi, N.F., Waldvogel, H.J., Tippett, L.J., Hogg, V.M., Synek, B.J., Faull, R.L.M., 2016. Symptom heterogeneity in Huntington's disease correlates with neuronal degeneration in the cerebral cortex. Neurobiol. Dis. 1 (96), 67–74.

Müller, H.P., Gorges, M., Grön, G., Kassubek, J., Landwehrmeyer, G.B., Süßmuth, S.D., et al., 2016. Motor network structure and function are associated with motor performance in Huntington's disease. J. Neurol. 263 (3), 539–549.

Myszczynska, M.A., Ojamies, P.N., Lacoste, A.M.B., Neil, D., Saffari, A., Mead, R., et al., 2020. Applications of machine learning to diagnosis and treatment of neurodegenerative diseases. Nat. Rev. Neurol. 16 (8), 440–456.

Nana, A.L., Kim, E.H., Thu, D.C.V., Oorschot, D.E., Tippett, L.J., Hogg, V.M., et al., 2014. Widespread Heterogeneous Neuronal Loss Across the Cerebral Cortex in Huntington's Disease. J Huntingt Dis. 3 (1), 45–64.
Niccolini, F., Politis, M., 2014. Neuroimaging in Huntington's disease. World J. Radiol. 6 (6), 301–312.
Novak, M.J.U., Seunarine, K.K., Gibbard, C.R., McColgan, P., Draganski, B., Friston, K., et al., 2015. Basal ganglia-cortical structural connectivity in Huntington's disease: Basal Ganglia-Cortical Connections in HD. Hum. Brain Mapp. 36 (5), 1728–1740.
Odish, O.F.F., Leemans, A., Reijntjes, R.H.A.M., van den Bogaard, S.J.A., Dumas, E.M., Wolterbeek, R., et al., 2015. Microstructural brain abnormalities in Huntington's disease: A two-year follow-up. Hum. Brain Mapp. 36 (6), 2061–2074.
Oliveira, A.S., Reiche, M.S., Vinescu, C.I., Thisted, S.A.H., Hedberg, C., Castro, M.N., et al., 2018. The cognitive complexity of concurrent cognitive-motor tasks reveals age-related deficits in motor performance. Sci. Rep. 8 (1), 6094.
Paulsen, J.S., 2009. Functional imaging in Huntington's disease. Exp. Neurol. 216 (2), 272–277.
Pini, L., Jacquemot, C., Cagnin, A., Meneghello, F., Semenza, C., Mantini, D., et al., 2020. Aberrant brain network connectivity in presymptomatic and manifest Huntington's disease: A systematic review. Hum. Brain Mapp. 41 (1), 256–269.
Pini, L., Youssov, K., Sambataro, F., Bachoud-Levi, A.C., Vallesi, A., Jacquemot, C., 2020. Striatal connectivity in pre-manifest Huntington's disease is differentially affected by disease burden. Eur. J. Neurol. 27 (11), 2147–2157.
Plummer, P., Eskes, G., Wallace, S., Giuffrida, C., Fraas, M., Campbell, G., et al., 2013. Cognitive-motor interference during functional mobility after stroke: state of the science and implications for future research. Arch. Phys. Med. Rehabil. 94 (12), 2565–2574.e6.
Poudel, G.R., Egan, G.F., Churchyard, A., Chua, P., Stout, J.C., Georgiou-Karistianis, N., 2014. Abnormal synchrony of resting state networks in premanifest and symptomatic Huntington disease: the IMAGE-HD study. Mar 1 [cited 2024 Oct 28]; 39(2). Available from: J. Psych. Neurosci. http://www.jpn.ca/lookup/doi/10.1503/jpn.120226.
Quarantelli, M., Salvatore, E., Cervo, A., Russo, C.V., Cocozza, S., Massarelli, M., et al., 2013. Default-mode network changes in huntington's disease: an integrated MRI study of functional connectivity and morphometry. PLoS One 8 (8).
Rolls, E.T., Cheng, W., Feng, J., 2020. The orbitofrontal cortex: reward, emotion and depression. Brain Commun. 2 (2), fcaa196.
Rosas, H.D., Salat, D.H., Lee, S.Y., Zaleta, A.K., Pappu, V., Fischl, B., et al., 2008. Cerebral cortex and the clinical expression of Huntington's disease: complexity and heterogeneity. Brain 131 (4), 1057–1068.
Soloveva, M.V., Jamadar, S.D., Poudel, G., Georgiou-Karistianis, N., 2018. A critical review of brain and cognitive reserve in Huntington's disease. Neurosci. Biobehav. Rev. 88, 155–169.
Soloveva, M.V., Jamadar, S.D., Hughes, M., Velakoulis, D., Poudel, G., Georgiou-Karistianis, N., 2020. Brain compensation during response inhibition in premanifest Huntington's disease. Brain Cogn. 1 (141), 105560.
Suzuki, A., Josselyn, S.A., Frankland, P.W., Masushige, S., Silva, A.J., Kida, S., 2004. Memory reconsolidation and extinction have distinct temporal and biochemical signatures. J. Neurosci. 24 (20), 4787–4795.
Tabrizi, S.J., Scahill, R.I., Owen, G., Durr, A., Leavitt, B.R., Roos, R.A., et al., 2013. Predictors of phenotypic progression and disease onset in premanifest and early-stage Huntington's disease in the TRACK-HD study: analysis of 36-month observational data. Lancet Neurol. 12 (7), 637–649.
Thobois, S., Ardouin, C., Lhommée, E., Klinger, H., Lagrange, C., Xie, J., et al., 2010. Non-motor dopamine withdrawal syndrome after surgery for Parkinson's disease: predictors and underlying mesolimbic denervation. Brain 133 (4), 1111–1127.
Thompson, J.C., Harris, J., Sollom, A.C., Stopford, C.L., Howard, E., Snowden, J.S., et al., 2012. Longitudinal evaluation of neuropsychiatric symptoms in Huntington's disease. J. Neuropsychiatry Clin. Neurosci. 8.
Thu, D.C.V., Oorschot, D.E., Tippett, L.J., Nana, A.L., Hogg, V.M., Synek, B.J., et al., 2010. Cell loss in the motor and cingulate cortex correlates with symptomatology in Huntington's disease. Brain J. Neurol. 133 (Pt 4), 1094–1110.
Tippett, L.J., Waldvogel, H.J., Thomas, S.J., Hogg, V.M., van Roon-Mom, W., Synek, B.J., et al., 2007. Striosomes and mood dysfunction in Huntington's disease. Brain J. Neurol. 130 (Pt 1), 206–221.
Tombaugh, T.N., 2004. Trail making test A and B: normative data stratified by age and education. Arch. Clin. Neuropsychol. 19 (2), 203–214.
Torrubia, R., Ávila, C., Moltó, J., Caseras, X., 2001. The Sensitivity to Punishment and Sensitivity to Reward Questionnaire (SPSRQ) as a measure of Gray's anxiety and impulsivity dimensions. Pers. Individ. Differ. 31 (6), 837–862.
Unschuld, P.G., Joel, S.E., Liu, X., Shanahan, M., Margolis, R.L., Biglan, K.M., et al., 2012. Impaired cortico-striatal functional connectivity in prodromal Huntington's Disease. Neurosci. Lett. 514 (2), 204–209.
van Duijn, E., Craufurd, D., Hubers, A.A.M., Giltay, E.J., Bonelli, R., Rickards, H., et al., 2014. Neuropsychiatric symptoms in a European Huntington's disease cohort (REGISTRY). J. Neurol. Neurosurg. Psychiatry 85 (12), 1411–1418.
Vinther-Jensen, T., Larsen, I.U., Hjermind, L.E., Budtz-Jørgensen, E., Nielsen, T.T., Nørremølle, A., et al., 2014. A clinical classification acknowledging neuropsychiatric and cognitive impairment in Huntington's disease [cited 2018 Dec 3];9(1). Available from: Orphanet. J. Rare Dis. http://ojrd.biomedcentral.com/articles/10.1186/s13023-014-0114-8.
Vonsattel, J.P.G., Myers, R.H., Stevens, T.J., Ferrante, R.J., Bird, E.D., Richardson Jr., E.P., 1985. Neuropathological classification of Huntington's disease. J. Neuropathol. Exp. Neurol. 44 (6), 559–577.
Vonsattel, J.P.G., Keller, C., Cortes Ramirez, E.P., 2011. Huntington's disease - neuropathology. Handb. Clin. Neurol. 100, 83–100.
Waldvogel, H.J., Thu, D., Hogg, V., Tippett, L., Faull, R.L.M., 2012. Selective neurodegeneration, neuropathology and symptom profiles in Huntington's disease. Adv. Exp. Med. Biol. 769, 141–152.
Waldvogel, H.J., Kim, E.H., Tippett, L.J., Vonsattel, J.P.G., Faull, R.L., 2014. The neuropathology of Huntington's disease. In: Nguyen, H.H.P., Cenci, M.A. (Eds.), Behavioral Neurobiology of Huntington's Disease and Parkinson's Disease. Springer Berlin Heidelberg, Berlin, Heidelberg [cited 2018 Dec 3]. p. 33–80. Available from: http://link.springer.com/10.1007/7854_2014_354.
Werner, C.J., Dogan, I., Saß, C., Mirzazade, S., Schiefer, J., Shah, N.J., et al., 2014. Altered resting-state connectivity in Huntington's Disease. Hum. Brain Mapp. 35 (6), 2582–2593.
Wolf, R.C., Sambataro, F., Vasic, N., Depping, M.S., Thomann, P.A., Landwehrmeyer, G.B., et al., 2014. Abnormal resting-state connectivity of motor and cognitive networks in early manifest Huntington's disease. Psychol. Med. 44 (15), 3341–3356.
Zeun, P., Scahill, R.I., Tabrizi, S.J., Wild, E.J., 2019. Fluid and imaging biomarkers for Huntington's disease. Mol. Cell. Neurosci. 97, 67–80.
Zhang, J., Gregory, S., Scahill, R.I., Durr, A., Thomas, D.L., Lehericy, S., et al., 2018. In vivo characterization of white matter pathology in premanifest Huntington's disease. Sep 15 [cited 2018 Oct 5]; Available from: Ann. Neurol. http://doi.wiley.com/10.1002/ana.25309.
Zhang, L., Pini, L., 2024. A divergent pattern in functional connectivity: a transdiagnostic perspective. Neural Regen. Res. 19 (9), 1885–1886.